Dual polarized high gain resonant cavity antenna (RCA) with a single layer metasurface for 6G applications

Mehrab Ramzan, and Padmanava Sen

Barkhausen Institut, Dresden, Germany
Email: {mehrab.ramzan, padmanava.sen}@barkhauseninstitut.org

***Abstract*—This paper presents a dual-polarized single layer metasurface in order to increase the gain of a single microstrip patch antenna in the X-band. The metasurface is comprised of circular unit cells with cross slots, exhibiting the same magnitude (S_{11} and S_{21}) and phase responses when subjected to TE and TM polarized waves. This single layer planar metasurface can boost the gain of a probe feed single microstrip patch antenna from 7.2 dBi to 16.2 dBi at 10 GHz. The antenna's gain and reflection coefficient with reference to the polarization of the antenna are made stable by employing cross slots, making it a more improved and robust design compared to the metasurface with rectangular slots. Moreover, a strong coupling is observed on the metasurface with cross slots considering both polarized waves.**

I. Introduction

In recent years, there has been a growing interest in integrated systems that can provide the capability of joint communication and sensing applications on the 6G platforms. In these integrated systems, the antenna is the main component at the leading RF front-ends, which require high gain antennas for sensing applications. The conventional techniques of developing an array of antennas require a complex transmission line network to operate and experience substrate losses at higher frequencies. Hence, there is a significant demand to explore new and simplified antenna solutions at higher frequencies to mitigate the free space path loss without increasing the costs. Metamaterials developed from basic unit cells are the best candidates that have numerous applications in the field of miniaturization of antennas [1], creating high isolation between TRx antennas [2], and high gain antennas [3]. However, they have polarization dependent properties [3].

This paper is an extension of our previous work [3], where a single layer metasurface with rectangular slots is used to increase the antenna's gain. Nevertheless, the metasurface presented is polarization dependent and does not have the same response if it is analyzed with respect to TE and TM waves. Therefore, the filtering abilities of the integrated antenna are reduced once the antenna's polarization is switched from horizontal to vertical. In this paper, a dual-polarized single layer metasurface is presented, showing the same magnitude and phase response to both polarized waves by using cross slots in the metasurface. The proposed dual-polarized metasurface is composed of circular unit cells with cross slots. In order to provide proof of the concept mentioned above, X-band (8-12 GHz), which can be the future 6G band, is used as the potential frequency band. The results are compared in terms of different polarization responses, gain, radiation efficiency, and aperture efficiency, and accordingly, the advantages of the new one layer metasurface are highlighted. It is shown that the cross slot can make the metasurface have identical results with respect to TE and TM polarized waves. The metasurface can increase the single element antenna gain from 7.2 dBi to 16.2 dBi and the gain of the antenna remains stable with respect to different orientations of the slots, making it a more robust design compared to the rectangular slot.

The following section is divided into two subsections. The first subsection provides a unit cell comparison of the single rectangular and cross slot. In the second subsection, the antenna is integrated with a new metasurface and the results are compared in terms of the reflection coefficient and the gain of the antenna. Finally, the conclusion of the paper is discussed.

This work is financed by the Saxon State government out of the State budget approved by the Saxon State Parliament.

DOI 10.23919/EuCAP57121.2023.10133153

II. Antenna and Metasurface

In this section, initially, the two metasurface unit cell simulations are compared. In the second subsection, the metasurfaces are integrated on top of a probe feed patch antenna and the results are compared in terms of the influence on the reflection coefficient, gain of the antenna and the surface current distribution on both metasurfaces.

A. Unit cell comparison

Both the metasurfaces, discussed in this subsection, are based on single layer 2D surfaces. One is based on rectangular slots and the other on cross slots in sub-wavelength circular patches, as shown in Fig. 1. In this subsection, the unit cell simulations of both designs are conducted and assessed in terms of their magnitude and phase responses when excited with TE and TM polarized waves as shown in Fig. 2. The optimized dimensions of both unit cells are given in Table I.

Fig. 3 shows the magnitude of the metasurface with rectangular slots with respect to TE and TM polarized waves. It is clearly shown that the magnitude response (S_{11} and S_{21}) of this metasurface is not the same and the reflection coefficient magnitude decreases with TM polarized wave, which results in lower directivity values of the antenna, evaluated according to equation 1. On the other hand, the metasurface with the cross slots has the same magnitude (S_{11} and S_{21}) response for both polarizations as shown in Fig. 4. The phase responses of both metasurfaces are shown in Fig. 5. The metasurface with cross slots has identical phase response which indicates that the metasurface will give similar results for both polarized waves if it is placed $\lambda/2$ away from the antenna surface, calculated using equation 2. The metasurface with rectangular slots does not show the same phase response for both polarizations, indicating that to achieve a desired performance, the metasurface should have distinct heights for both polarized waves, computed using equation 2.

$$D = 10\log\frac{1+|\Gamma|}{1-|\Gamma|} \quad (1)$$

$$h1 + t\sqrt{\epsilon_r} = \frac{(\Phi_m + \phi_g)\lambda}{4\pi} + \frac{N\lambda}{2} \qquad N = 0, \pm1, \pm2, .. \quad (2)$$

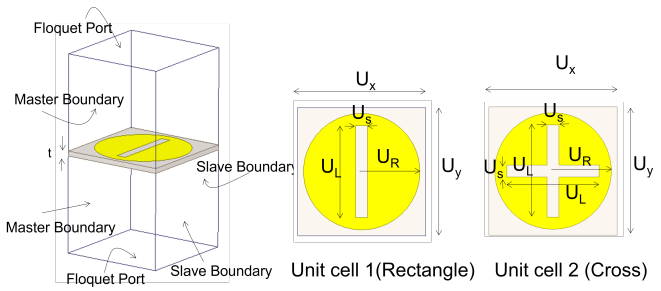

Fig. 1. Highlighted dimensions of unit cell 1 (rectangular slot) and unit cell 2 (cross slot)

TABLE I
DIMENSIONS OF UNIT CELL 1 (RECTANGULAR SLOT) AND UNIT CELL 2 (CROSS SLOT)

Parameters	Unit cell 1 (mm)	Unit cell 2 (mm)
U_x	10.635	10.635
U_y	10.635	10.635
U_s	0.9	0.9
U_L	7.65	7.65
U_R	4.84	4.84
t	0.508	0.508

B. Comparison of metasurfaces

In this subsection, both metasurfaces are integrated with a single patch probe feed antenna at a height (h1) of $\lambda/2$, as shown in Fig. 6. The results are compared in terms of different cases of slot orientations with respect to the antenna, as shown in Fig. 7 and 8, respectively. In order to make a fair comparison

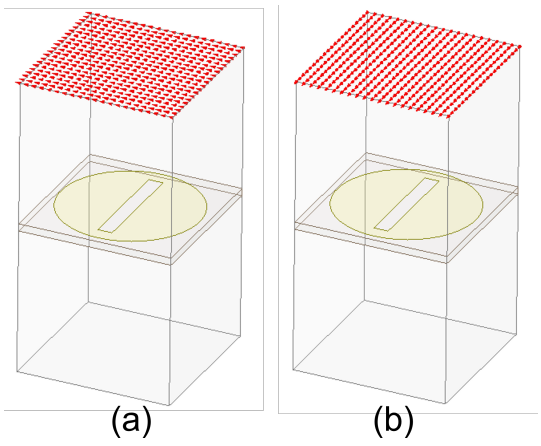

Fig. 2. Different excited modes of floquet ports in HFSS EM environment (a) TE (b) TM modes

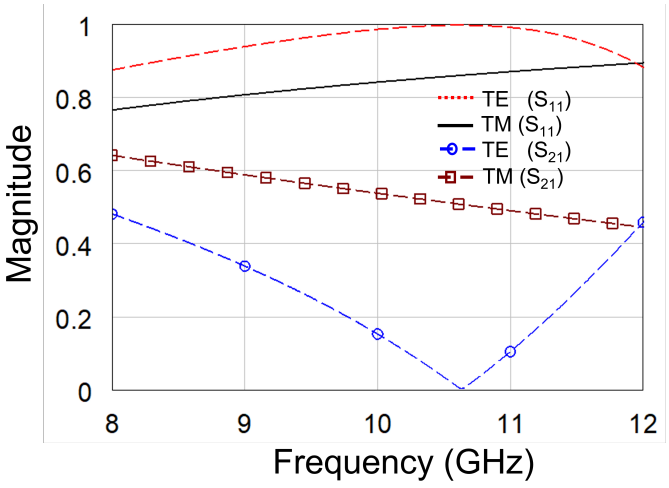

Fig. 3. Magnitude response of the metasurface with the rectangular slots

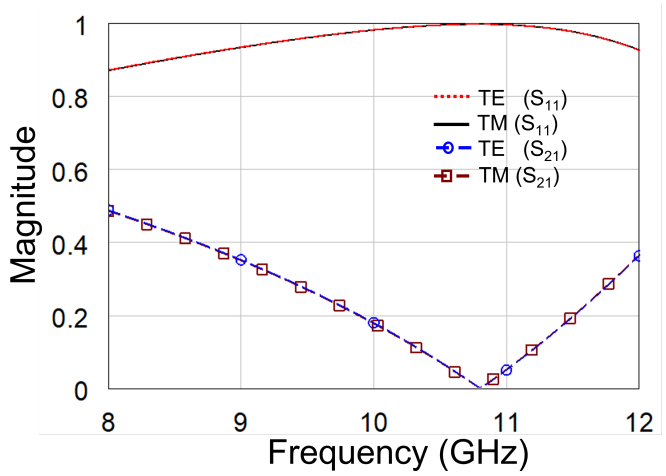

Fig. 4. Magnitude response of the metasurface with the cross slots

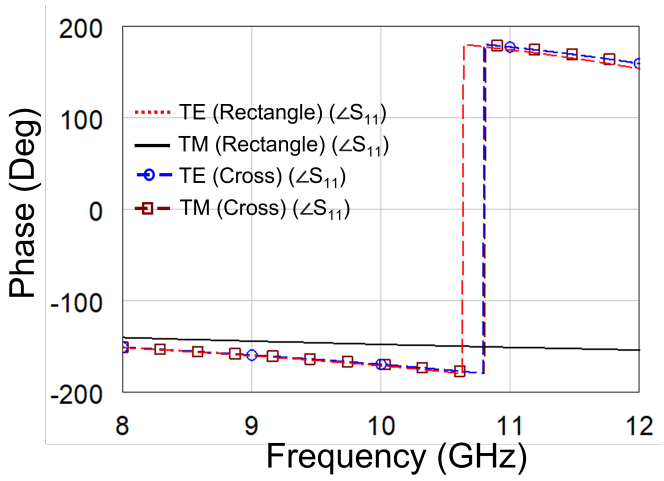

Fig. 5. Comparison of the Phase response of the metasurfaces with respect to TE and TM polarized waves

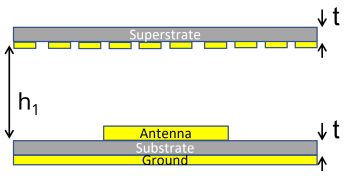

Fig. 6. Integration of the metasurface with the microstrip patch antenna

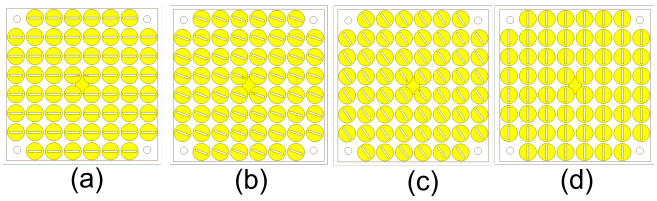

Fig. 7. Different cases of rectangular slot orientation with respect to the antenna (a) 0° (b) 35° (c) 70° (d) 90°

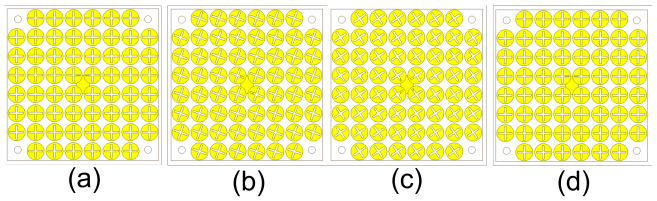

Fig. 8. Different cases of cross slot orientation with respect to the antenna (a) 0° (b) 35° (c) 70° (d) 90°

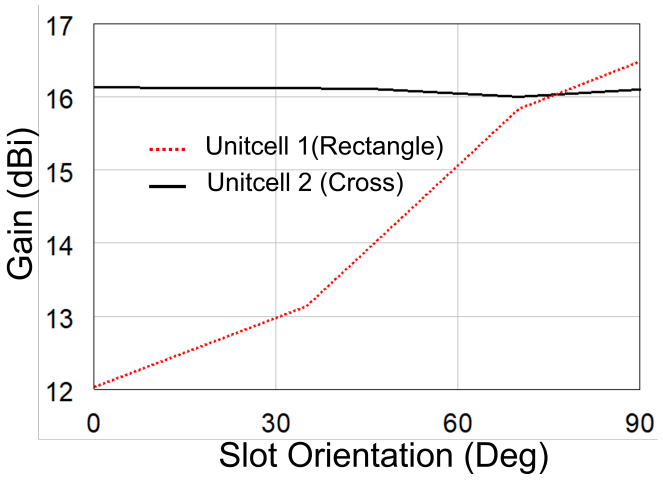

Fig. 9. Gain comparison of the two metasurfaces with respect to the rotation of the corresponding slots

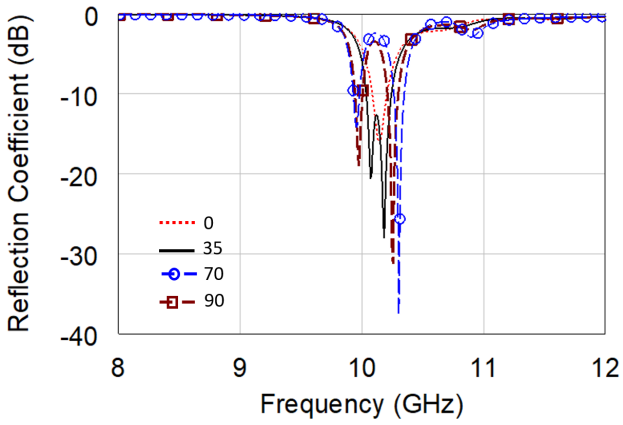

Fig. 10. Reflection coefficient response of the antenna corresponding to the orientation of the rectangular slot (unit cell 1) of the metasurface

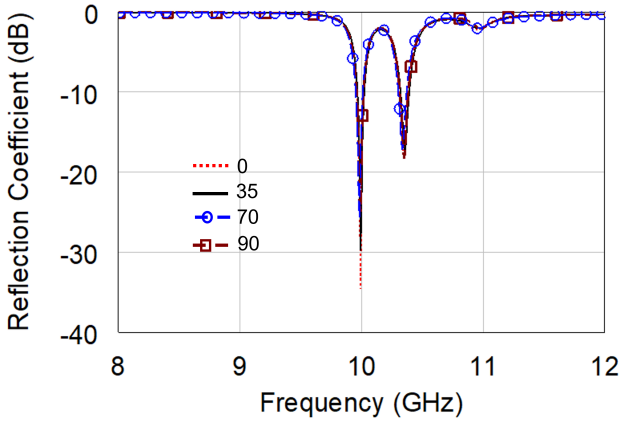

Fig. 11. Reflection coefficient response of the antenna corresponding to the orientation of the cross slot (unit cell 2) of the metasurface

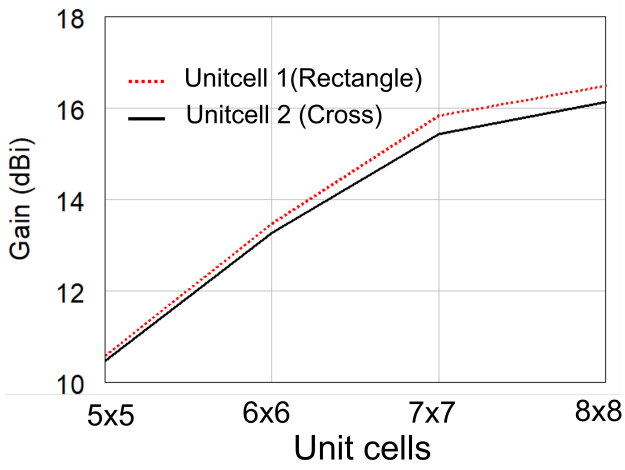

Fig. 12. Gain comparison of the two metasurfaces with respect to different unit cells

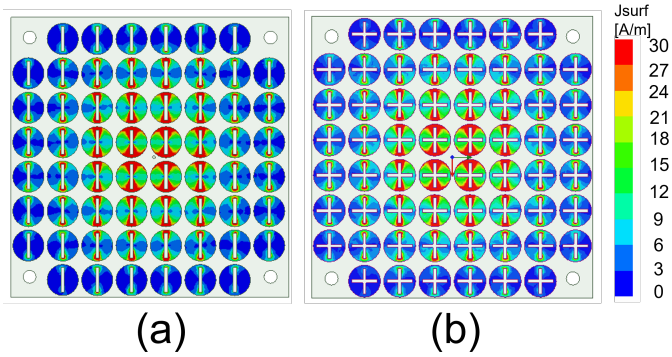

Fig. 13. Current distribution plots on the metasurface with (a) Unit cell 1 (rectangular slots orientation 90°) (b) Unit cell 2 (cross slots orientation 90°) at 10 GHz

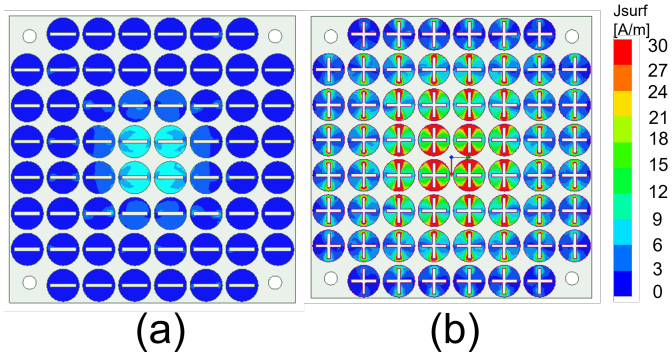

Fig. 14. Current distribution plots on the metasurface with (a) Unitcell 1 (rectangular slots orientation 0°) (b) Unitcell 2 (cross slots orientation 0°) at 10 GHz

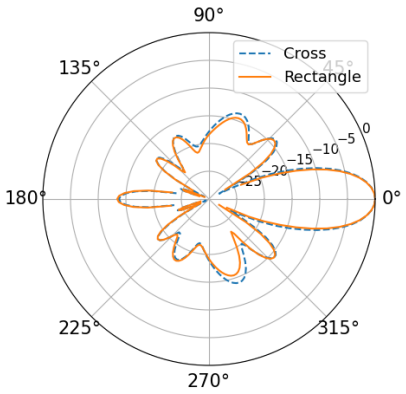

Fig. 15. Radiation pattern comparison of the metasurfaces with rectangular and cross slots in the E-Plane at 10 GHz

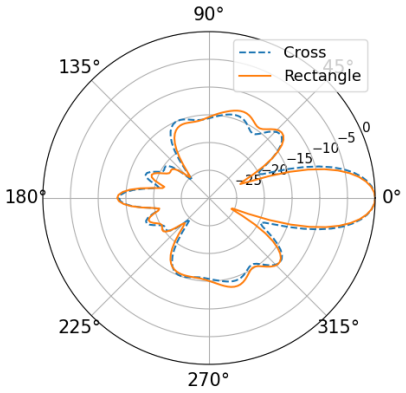

Fig. 16. Radiation pattern comparison of the metasurfaces with rectangular and cross slots in the H-Plane at 10 GHz

between the two designs, the metasurfaces are designed on the same substrate material (RO4350B) with a thickness of 0.508 mm, and the size (86 mm x 86 mm) of the metasurface is kept the same containing an equal number of unit cells in the x and y-direction. Fig 9 shows the gain comparison of both metasurfaces with respect to the slots rotated with reference to the antenna polarization. The results clearly indicate that the metasurface with the rectangular slots has dependent gain and becomes maximum when it is perpendicular to the excited antenna. In contrast, the metasurface with cross slots shows almost constant gain even when the cross slot is rotated with respect to the orientation of the excited microstrip patch antenna.

Furthermore, the reflection coefficient of the two antennas with different metasurfaces is also compared. The reflection coefficient of the metasurface with the rectangular slots has a varying response, as shown in Fig. 10. On the other hand, the metasurface with cross slots has a negligible effect on the antenna's input reflection coefficient while having the same response for both polarized waves as shown in Fig. 11.

In addition to the slot orientations, the gain of the antennas is also investigated with respect to the size of the metasurface

TABLE II
COMPARISON OF THE SINGLE LAYER METASURFACE BASED ANTENNA WITH THE OTHER PUBLISHED ARTICLES

Ref.	Feed	Size (λ_0)	BW (%)	M.Gain (dBi)	SLL (dB)	HPBW	Rad. Eff.	App. Eff.	Dual P	L
[3]	Probe	2.83 x 2.83 x 0.5	0.55+0.78	16.5	<-13	18°	91.38	44.38	No	1
[4]	1 Patch	4.43 x 4.43 x 0.062	3.15	15.8	NA	30°	NA	15.4	No	2
[5]	WG slot	1.9 x 1.9 x 0.5	21.5	16.1	NA	NA	-	78.6	No	2
[6]	WG slot	2.4 x 2.4 x 0.66	-	14	-18	>30°	NA	34.6	-	4
[7]	2x2 Array	1.55 x 1.55 x 0.11	24.3	12.5	-20	NA	-	53.7	-	2
[8]	2x2 Array	2.8 x 2.8 x 0.5	26.9	15.7	<-10	25°	86.8	37.7	-	2
[9]	Ms Slot	2.2 x 2.2 x 0.54	25	13.92	-	-	-	40.5	-	2
[10]	Ms Slot	2.76 x 2.76 x 0.5	15.5	13.78	-	-	-	25	-	2
This Work	Probe	2.83 x 2.83 x 0.5	0.55+0.78	16.2	<-13	18°	87.5	40.5	Yes	1

λ_0 Center frequency wavelength, ^{WG} Waveguide, ^{Ms} Microstrip,^{BW} -10 dB Impedance bandwidth, ^{SLL} Side lobe level, ^{HPBW} Half power beam width, $^{Rad.Ef.}$ Radiation Efficiency (%), $^{App.Ef.}$ Aperture Efficiency (%), $^{DualP.}$ Dual polarization, ^{L} Layers

containing 5x5 to 8x8 unit cell elements. The comparison is shown in Fig. 12, where both metasurfaces show the same increasing trend with respect to the growing size of the metasurface. However, few differences are observed when the metasurface size is more prominent; the metasurface with the cross slots shows a bit lower gain due to the introduction of an extra slot. A comparison between the surface current distribution shows identical directive behavior in the broadside direction, maximum at the center and decaying at the edges of the metasurface, as shown in Fig. 13. On the other side, the coupling on metasurface with rectangular slots becomes significantly less if the slots are rotated 0° with reference to the antenna polarization whereas the metasurface with cross slots keeps its current distribution preserved as shown in Fig. 14. Moreover, the radiation patterns of both antennas are compared in the E-plane and H-plane at 10 GHz. The corresponding results are shown in Fig. 15 and Fig. 16, respectively. The results clearly demonstrate that both antennas (metasurfaces with rectangular and cross slots) have identical radiation patterns in both planes. Therefore, the metasurface with cross slots is the ideal candidate that not only preserves the radiation pattern but also keeps the input reflection coefficient of the antenna stable with both polarized waves.

Finally, a review of recent literature comparing the different metasurface based antennas is shown in Table II. The proposed metasurface design has fewer fabrication complexities with only one layer and the additional capability of operating in dual polarized mode. However, the antenna's radiation efficiency is decreased with respect to the rectangular slots due to the introduction of a new slot, but it still remains above 87 %.

III. CONCLUSIONS

This paper compares two single-layer metasurfaces based on rectangular and cross slots in sub-wavelength circular unit cells. The cross slot metasurface shows more stable behavior in terms of gain and reflection coefficient when analyzed with respect to TE and TM polarized waves. These studies can be further extended to check the response with circular polarized antennas. As future work, the proposed design will be fabricated and integrated with real antennas for performance analysis. More investigation is required to combine the two resonances in order to increase and make the bandwidth continuous across the application band.

ACKNOWLEDGEMENT

This work is financed on the basis of the budget passed by the Saxon State Parliament. The authors would like to acknowledge the contribution of Tim Hentschel and Gerhard Fettweis to this work.

REFERENCES

[1] S. Ahdi Rezaeieh, M. A. Antoniades, and A. M. Abbosh, "Miniaturization of planar yagi antennas using mu-negative metamaterial-loaded reflector," *IEEE Transactions on Antennas and Propagation*, vol. 65, no. 12, pp. 6827–6837, 2017.

[2] M. Ramzan, A. N. Barreto, and P. Sen, "Meta-surface boosted antenna to achieve higher than 50 db trx isolation at 26 ghz for joint communication and radar sensing (jc&s)," in *2022 16th European Conference on Antennas and Propagation (EuCAP)*, 2022, pp. 1–5.

[3] M. Ramzan and P. Sen, "Dual-band gain-boosted planar lens antenna using a single layer metasurface for 6g applications," in *2022 Joint European Conference on Networks and Communications & 6G Summit (EuCNC/6G Summit)*, 2022, pp. 446–450.

[4] A. Ghasemi, S. N. Burokur, A. Dhouibi, and A. de Lustrac, "High beam steering in fabry–pérot leaky-wave antennas," *IEEE Antennas and Wireless Propagation Letters*, vol. 12, pp. 261–264, 2013.

[5] A. Lalbakhsh *et al.*, "Single-dielectric wideband partially reflecting surface with variable reflection components for realization of a compact high-gain resonant cavity antenna," *IEEE Transactions on Antennas and Propagation*, vol. 67, no. 3, pp. 1916–1921, 2019.

[6] M. W. Niaz *et al.*, "Wideband fabry–perot resonator antenna employing multilayer partially reflective surface," *IEEE Transactions on Antennas and Propagation*, vol. 69, no. 4, pp. 2404–2409, 2021.

[7] S. Jagtap *et al.*, "A wideband microstrip array design using ris and prs layers," *IEEE Antennas and Wireless Propagation Letters*, vol. 17, no. 3, pp. 509–512, 2018.

[8] C. Yang, X.-W. Zhu, and P. Liu, "A circularly polarized fabry-perot resonant cavity antenna using frequency selective surface-based partial reflecting surface," *International Journal of RF and Microwave Computer-Aided Engineering*, p. e22735, 2021.

[9] F. Meng and S. K. Sharma, "A wideband resonant cavity antenna with compact partially reflective surface," *IEEE Transactions on Antennas and Propagation*, vol. 68, no. 2, pp. 1155–1160, 2020.

[10] M. A. Meriche *et al.*, "Directive wideband cavity antenna with single-layer meta-superstrate," *IEEE Antennas and Wireless Propagation Letters*, vol. 18, no. 9, pp. 1771–1774, 2019.